https://doi.org/10.5194/nhess-2021-287
Preprint. Discussion started: 21 October 2021

Natural Hazards and Earth System Sciences
Discussions

Brief Communication: A case study of risk assessment for facilities associated with earthquake-induced liquefaction potential in Kimhae City, South Korea

Sang-Soo Jeon[1], Daeyang Heo[2], Sang-Seung Lee[3]

[1] Department of Civil & Urban Engineering, Construction Technology Research Center, INJE University, Inje-ro 197, Kimhae City, Gyeongsangnam-do, 50834, South Korea

[2]Industrial Site Division, Gyeongsangnam-do Provincial Government, 200 Jungangdae-ro, Uichang-gu, Changwon City, Gyeongsangnam-do, 51154, South Korea

[3]Kyong-Ho Engineering, Kyongho Building, 41 Cheyukgwan-ro 74 Beon-gil, Guri, Gyeonggi-Do, 11940, South Korea

Correspondence to: Sang-Soo Jeon (ssj@inje.ac.kr)

Abstract Liquefaction causes secondary damage after earthquakes; however, liquefaction related phenomena were rarely reported until after the M_w = 5.4 November 15, 2017 Pohang earthquake in Korea. Both the M_w = 5.8 September 12, 2016 Gyeongju earthquake and M_w = 5.4 November 15, 2017 Pohang earthquake occurred in the fault zone of Yangsan City (located in the south-eastern part of South Korea), and both of these earthquakes induced liquefaction. Moreover, they demonstrated that Korea is not safe against the liquefaction induced by earthquakes. In this study, estimations and calculations were performed based on the distances between the centroids of administrative districts and an epicenter located at the Yangsan Fault, the peak ground accelerations (PGAs) induced by M_w = 5.0 and 6.5 earthquakes, and a liquefaction potential index (LPI) calculated based on groundwater level and standard penetration test results from 274 locations in Kimhae City (adjacent to the Nakdong river and across the Yangsan Fault). Then, a kriging method using geographical information systems was used to evaluate the liquefaction effects on the risk levels of facilities. The results indicate that a M_w = 5.0 earthquake induces a small and low level of liquefaction, resulting in slight risk for facilities, but a M_w = 6.5 earthquake induces a large and high level of liquefaction, resulting in a severe risk for facilities.

1 Introduction

Soil liquefaction occurs when the strength of soils (in areas with a high level of groundwater and loose sand or sandy soils) is reduced by applied earthquake loading. A loss of shear strength occurs because the effective stress is reduced as excess pore water pressure is increased and gradually decreased when earthquake loading is applied (Kramer, 1996; Youd and Idriss, 2001).

The soil liquefaction induced by the Pohang earthquake was reported as a first case in Korea; however, liquefaction has occurred following various earthquakes, including the Niigata earthquake (M_w = 7.6) in 1964, Loma Prieta earthquake (M_w = 6.9) in 1989, Northridge earthquake (M_w = 6.7) in 1994, Tohoku earthquake (M_w = 9.1) in 2011, and Christchurch earthquakes (M_w = 6.2–7.1) in 2010 and 2011. Earthquakes resulted in substantial amounts of infrastructure damage, such as building damage induced by differential settlements, the lateral displacement of roads, and lifeline damage. The structural and foundation performances of facilities subjected to settlement and tilt when subsurface layers of soils are liquefiable have been analyzed to estimate the resulting damage (Bakir and Karasin, 2016; Bray and Dashti, 2010; Bullock et al., 2019; Hayden, 2014; Kamao et al., 2014; Lanzano et al., 2014; Lu et al., 2017; Wakamatsu and Numata, 2004; Zupan, 2014). Other studies have constructed soil liquefaction hazard maps to determine land damage and/or analyze liquefaction potential (Ballegooy et al., 2012; Habibullah et al., 2012; Naik et al., 2020; Ziabari et al., 2017).

A liquefaction potential index (LPI) has also been used to estimate the risk levels of facilities with respect to liquefaction (Holzer, 2008; Iwasaki et al., 1982). The LPI is based on a factor of safety (FS) calculated based on the

https://doi.org/10.5194/nhess-2021-287
Preprint. Discussion started: 21 October 2021

groundwater level and peak ground acceleration (PGA) induced by earthquake loading, and it represents the liquefaction potential. There is no liquefaction when the FS is equal to or greater than 1.0; by contrast, it has the potential for liquefaction when the FS is less than 1.0. However, a liquefaction potential estimated using the FS cannot represent the ground damage for broad areas; rather, it is only applicable to local specific areas. The LPI proposed by Iwaski et al. (1982) has been used to estimate the hazards induced by liquefaction in broad areas and to produce corresponding hazard maps (Chung and Rogers, 2011; Iwasaki et al., 1982; Lee et al., 2003).

When an earthquake occurs, the liquefaction potential is determined by the groundwater level and PGA associated with the ground characteristics. In this study, the safety of facilities in Kimhae City (located in the south-eastern part of Korea) was estimated based on attenuation equations associated with the distance from the epicenter to the centroid of seventeen administrative districts in Kimhae City. The Pohang earthquake, the largest recent earthquake in Korea, had a magnitude of 5.0. An earthquake magnitude of 6.5, corresponding to a PGA of 0.2g, is the standard for the design of earthquake-resistant structures in Korea. Therefore, in this study, the FS values for facilities in Kimhae City were estimated for M_w 5.0- and 6.5-earthquakes, and the liquefaction potential was evaluated based on currently available standard penetration test (SPT) results. Since cone penetration test (CPT) results can reflect more precise ground conditions, in the future, liquefaction potential values should be revised based on CPT results to estimate the risk levels of facilities. Moreover, attenuation relationships should be developed to reflect the widely distributed transgressive sands in Kimhae City.

2 Liquefaction Potential Index (LPI)

In this study, the LPI proposed by Iwasaki et al. (1978) was used to estimate the ground damage level induced by liquefaction. As described in Eqn. (1), the LPI is calculated based on the ground depth and characteristics of soil, as follows:

$$\mathrm{LPI} = \int_0^{20} F(z)W(z)dz \quad (1)$$

In this equation, z represents the ground depth, and F(z) is a function of the FS for liquefaction. If FS ≤ 1.0, F(z) = (1- FS), and if FS > 1.0, F(z) = 0. W(z) = (10 – 0.5 z) and W(z) = 0 for z ≤ 20 m and z > 20 m, respectively. Eqn. (1) provides LPIs in the range from 0 to 100. Iwasaki et al. (1978) proposed levels of liquefaction severity, as described in Table 1, associated with 63 and 22 areas at liquefaction and non-liquefaction sites, respectively.

Table 1. Level of liquefaction severity based on liquefaction potential index (LPI) (Iwasaki et al., 1982)

LPI	Severity
0	Very low
0 < LPI ≤ 5	Low
5 < LPI ≤ 15	High
15 < LPI	Very high

The LPI is determined by integrating F(z) multiplied by W(z) from the ground surface to a ground depth of 20 m, and a single value corresponding to a site is evaluated. The LPI can be evaluated for each layer of soil. For example, if a non-liquefaction layer such as bed rock exists in the soil layers within 20 m of ground depth, the ground depth for calculating the LPI is estimated from the ground surface to the depth susceptible to liquefaction.

A simplified method for estimating the FS of liquefaction was proposed by Seed and Idriss (1971), as follows:

$$\mathrm{FS} = \frac{\mathrm{CRR}}{\mathrm{CSR}} \times \mathrm{MSF} \quad (2)$$

The cyclic resistance ratio (CRR) and cyclic stress ratio (CSR) represent the capacity of soil to resist liquefaction and the ratio of the shear stress relative to the effective vertical overburden stress, respectively. The magnitude scaling factor (MSF) varies with the magnitude of the earthquake. In this study, as shown in Figure 1, a flowchart is used to determine the LPI values. The CSR and CRR are calculated based on the SPT results and soil parameters, respectively.

https://doi.org/10.5194/nhess-2021-287
Preprint. Discussion started: 21 October 2021

Natural Hazards and Earth System Sciences
Discussions

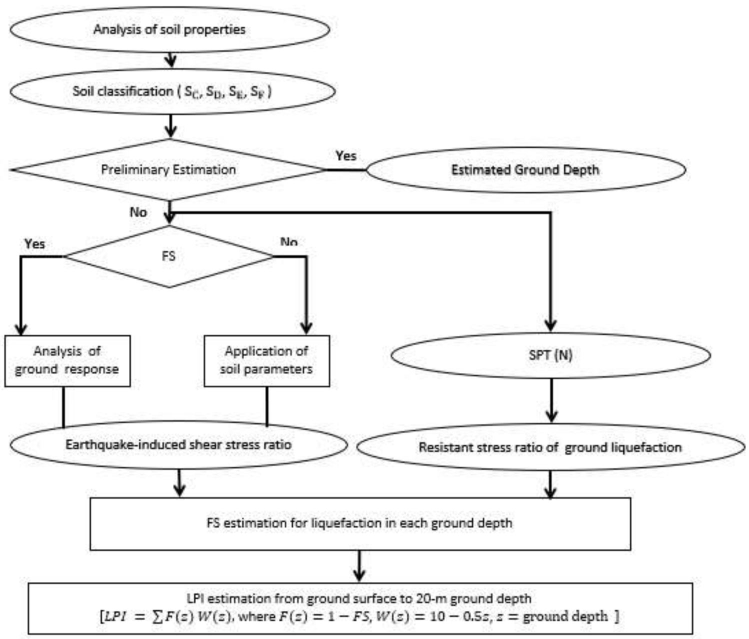

Figure 1. Flowchart for estimating liquefaction potential index (LPI) (Choe and Ku, 2009)

3 Estimation of peak ground acceleration (PGA)

The PGA induced by an earthquake has large variations associated with the soil characteristics, distance from the epicenter, and ground depth. As the PGA is a crucial factor, it is directly used to evaluate earthquake-induced damage. The largest PGA normally occurs near the epicenter, and the PGA generally decreases as the distance from the epicenter increases. In this study, the PGA was evaluated based on both the distance from each administrative district to the epicenter and an attenuation relationship; then, the risk levels of facilities affected by earthquake-induced liquefaction were evaluated.

3.1 Estimation of the location of epicenter and distance from epicenter to each administrative district

Figure 2 shows Kimhae City with respect to the active Yangsan Fault. As shown in Figure 2(a), the fault lies across the study area (Kimhae City), and the horizontally extended location from the centroid of Kimhae City to the closest fault is assumed to be the location of the epicenter. The distance from the centroid of Kimhae City to the epicenter is 16.8 km. There are seventeen administrative districts in Kimhae City. The distances from the epicenter to the centroid of each administrative district were calculated. Figure 2(b) shows an example of how the distance of 3.6 km from Daedong-myun to the epicenter was calculated. Table 2 describes the distances from the centroid of each administrative district to the epicenter.

https://doi.org/10.5194/nhess-2021-287
Preprint. Discussion started: 21 October 2021

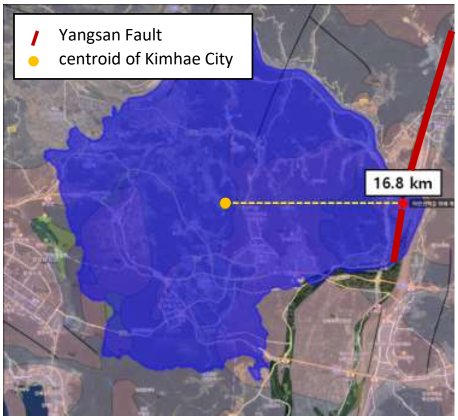

(a) Distance from epicenter to the centroid of Kimhae City

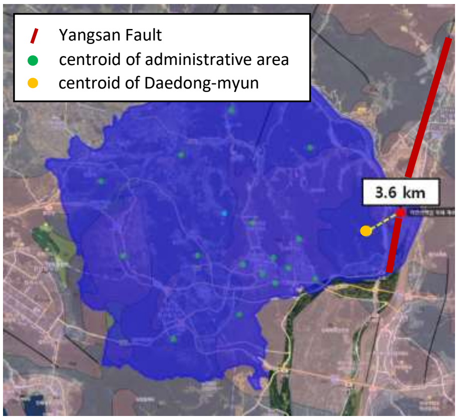

(b) Distance from epicenter to the centroid of Daedong-myun

Figure 2. Distance from epicenter to the centroid of Kimhae City and Daedong-myun, respectively.

https://doi.org/10.5194/nhess-2021-287
Preprint. Discussion started: 21 October 2021

Table 2. Distance from Yangsan Fault to centroid of each administrative district

Administrative district	Distance from Yangsan fault (km)
Daedong-myeon	3.6
Saman-dong	10.1
Buram-dong	10.3
Sangdong-myeon	10.6
Hwalcheon-dong	11.9
Dongsang-dong	12.8
Buwon-dong	13.8
Bukbu-dong	14.2
Hoehyeon-dong	14.5
Chilsanseobu-dong	18.1
Naeoe-dong	18.8
Saengnim-myeon	18.8
Juchon-myeon	19.8
Hallim-myeon	21.7
Jangyu-myeon	24.8
Jillye-myeon	27.0
Jinyeong-eup	28.7

3.2 Attenuation relationship of PGA

Three of the most reliable attenuation relationships for the PGA have been proposed for use by the Ministry of the Interior and Safety of Korea (Choi et al., 2005; Jo and Baag, 2003; Lee et al., 2003). The most reliable attenuation relationship proposed by Choi et al. (2005) was used in this study. The attenuation relationship proposed by Choi et al. (2005) is compared to those proposed by Midorikawa (2004) and Munson (1997) for an earthquake magnitude of 5.0; it is found that the PGAs obtained from the attenuation relationship proposed by Choi et al. (2005) are highly similar to those obtained from the relationship proposed by Midorikawa (2004), but different from those obtained from Munson (1997), with the latter being based on ground conditions in Hawaii. As the calculated values are shown in Figure 3, as there were no available data corresponding to a distance of less than 10 km and the attenuation relationship proposed by Choi et al. (2005) resulted in the overprediction of the PGAs. Therefore, the attenuation relationship was considered as unreliable within a 10-km distance from the epicenter. Eqn. (3) expresses the attenuation relationship proposed by Choi et al. (2005), and Table 3 describes the parameters of the attenuation relationship for estimating PGAs.

$$lnPGA\left(\frac{cm}{sec^2}\right) = c_0 + c_1 R + c_2 lnR - \ln[\min(R, 100)] - \frac{1}{2}\ln[\max(R, 100)] \quad (3)$$

In the above, R represents the distance from the epicenter, and $c_k(0,1,2) = \xi_0^k + \xi_1^k(M_w - 6) + \xi_2^k(M_w - 6)^2 + \xi_3^k(M_w - 6)^3$ for k = 0, 1, and 2.

https://doi.org/10.5194/nhess-2021-287
Preprint. Discussion started: 21 October 2021

Table 3. Parameters of the attenuation relationship for estimating PGA (Jo and Baag, 2003)

	ξ_0^0	ξ_0^1	ξ_0^2	ξ_1^0	ξ_1^1	ξ_1^2	ξ_2^0	ξ_2^1	ξ_2^2	ξ_3^0	ξ_3^1	ξ_3^2
PGA	0.1073829 E+02	-0.2379955 E-02	-0.2437218 E+00	0.5909022 E+00	0.2081359 E-03	0.9498274 E-01	-0.5622945 E-01	-0.2046806 E-04	-0.8804236 E-02	0.2135007 E-01	0.4192630 - E-04	-0.3302350 E-02

The SPT data of 903 locations, provided by both the geotechnical information database system of a governmental organization and construction companies, were collected to estimate the LPI values in the study area. Since some of the important SPT data were missing, a reliable dataset of 274 locations was selected, and then a geographical information system was used to plot the locations of the selected SPT data. The locations of SPT linearly arrayed inside of the dotted line may result in the deviation of contour lines of LPI as shown in Figure 4. The SPT data recorded at the various coordinates and the kriging method were used to construct the contour lines of the LPI values.

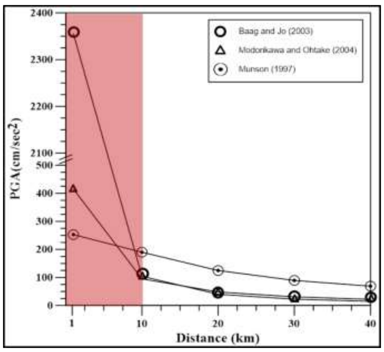

Fig. 3. Peak ground acceleration (PGA) vs. distance from epicenter

Fig. 4. Location of standard penetration test (SPT) used to estimate LPI

4 Risk level of facilities in Kimhae City

Facilities in Kimhae City are categorized as described in Table 4.

Table 4. Facilities in Kimhae City

Facility	Number or length
Tunnel	15
Bridge	412
Light rail transit (km)	24.6km
Railway (km)	91.3km
Road (km)	1,145.3km
Water pipe (km)	1,340.0km
Sewage pipe (km)	1,502.0km
Public facility	96,729
Shelter outside a building	27

https://doi.org/10.5194/nhess-2021-287
Preprint. Discussion started: 21 October 2021

Natural Hazards and Earth System Sciences
Open Access
EGU
Discussions

4.1 Spatial distribution of LPI for M_w = 5.0 and 6.5 earthquakes

Figures 5(a) and (b) show the LPI distribution and Figures 5(c) and (d) show the ratio of the covered area with respect to the range of the LPI values for M_w = 5.0 and 6.5 earthquakes, respectively.

The "very high" and "high" level of liquefaction severity for the M_w = 5.0 earthquake cover 2 km^2 (0.2%) and 22.1 km^2 (4.8%) of the study area, respectively. The "very high" and "high" level of liquefaction severity for the M_w = 6.5 earthquake cover 28.6 km^2 (6.2%) and 11.5 km^2 (2.5%) of the study area, respectively. These areas seem to be small in proportion to the total area, but are not small in proportion to the plat area. As the earthquake magnitude increases from M_w = 5.0 to M_w = 6.5, the proportion of land with high level of liquefaction severity increases substantially.

Figure 6 shows bridges, buildings, and water pipelines superimposed on the spatial distribution of the LPI for both the M_w = 5.0 and 6.5 earthquakes. Figure 7 shows how facilities are distributed in level of liquefaction severity zones. As we expected, much greater proportions of facilities are distributed in high level of liquefaction severity areas for the M_w = 6.5 earthquake relative to those for the M_w = 5.0 earthquake.

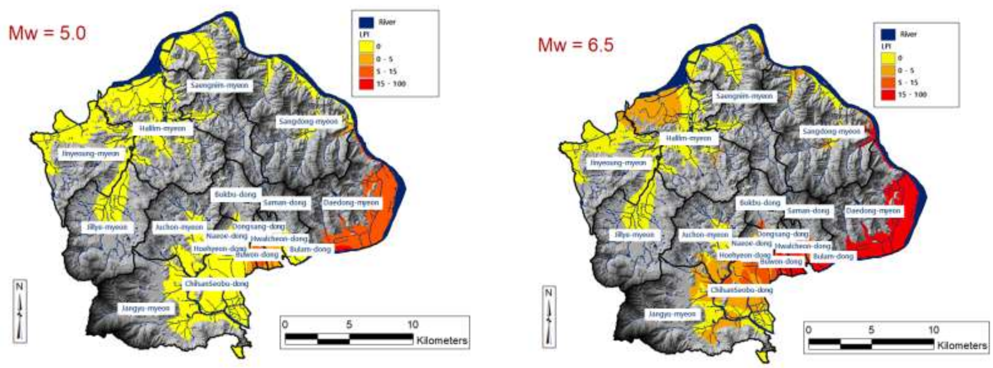

(a) Spatial distribution of LPI for M_w = 5.0 earthquake (b) Spatial distribution of LPI for M_w = 6.5 earthquake

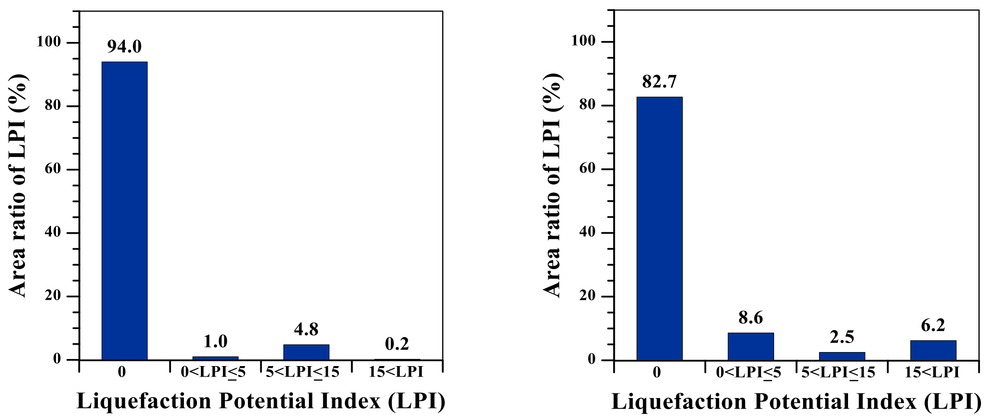

(c) Area ratio of LPI for M_w = 5.0 earthquake (d) Area ratio of LPI for M_w = 6.5 earthquake

Figure 5. Spatial distribution and area ratio of LPI for M_w = 5.0 and 6.5 earthquakes, respectively

https://doi.org/10.5194/nhess-2021-287
Preprint. Discussion started: 21 October 2021

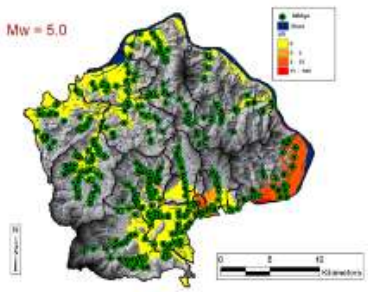

(a) Bridges superimposed on spatial distribution of LPI for $M_w = 5.0$ earthquake

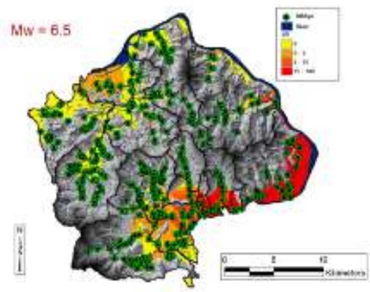

(b) Bridges superimposed on spatial distribution of LPI for $M_w = 6.5$ earthquake

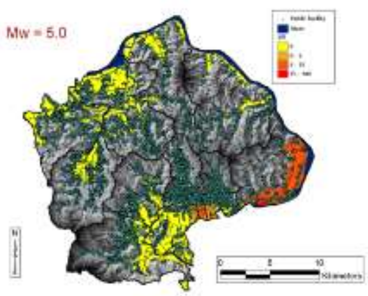

(c) Public facilities superimposed on spatial distribution of LPI for $M_w = 5.0$ earthquake

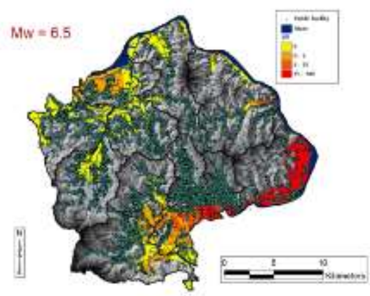

(d) Public facilities superimposed on spatial distribution of LPI for $M_w = 6.5$ earthquake

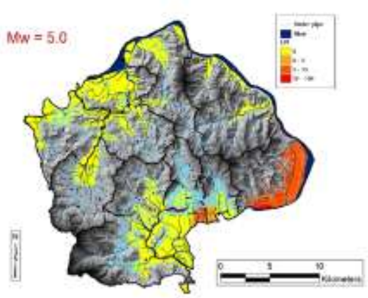

(e) Water pipelines superimposed on spatial distribution of LPI for $M_w = 5.0$ earthquake

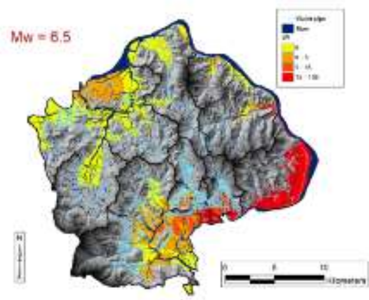

(f) Water pipelines superimposed on spatial distribution of LPI for $M_w = 6.5$ earthquake

Figure 6. Bridges, buildings, and water pipelines superimposed on spatial distribution of LPI for $M_w = 5.0$ and 6.5 earthquakes, respectively

https://doi.org/10.5194/nhess-2021-287
Preprint. Discussion started: 21 October 2021

Natural Hazards and Earth System Sciences
Discussions

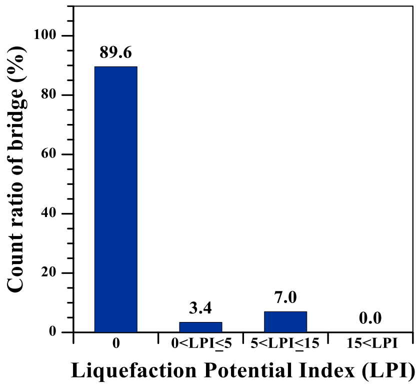

(a) Bridges with respect to LPI for $M_w = 5.0$ earthquake

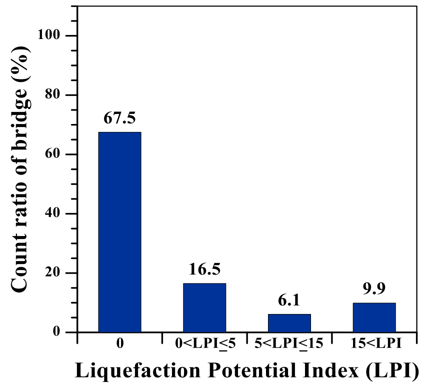

(b) Bridges with respect to LPI for $M_w = 6.5$ earthquake

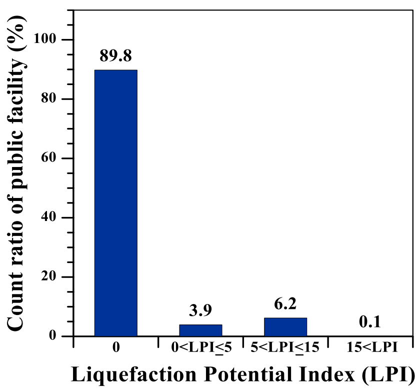

(c) Public facilities with respect to LPI for $M_w = 5.0$ earthquake

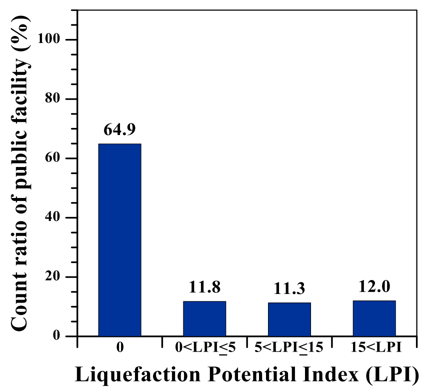

(d) Public facilities with respect to LPI for $M_w = 6.5$ earthquake

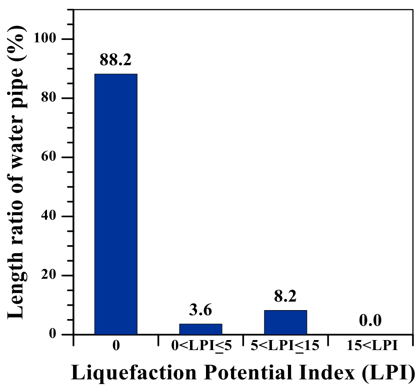

(e) Water pipelines with respect to LPI for $M_w = 5.0$ earthquake

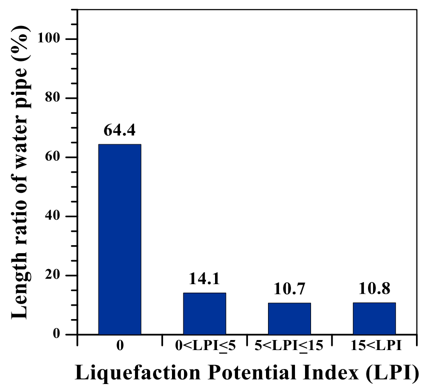

(f) Water pipelines with respect to LPI for $M_w = 6.5$ earthquake

Figure 7. Bridges, buildings, and water pipeline with respect to LPI for M_w = 5.0 and 6.5 earthquakes.

Natural Hazards and Earth System Sciences
Open Access
EGU
Discussions

4.2 Risk assessment of facilities with respect to LPI for M_w = 5.0 and M_w = 6.5 earthquakes

In general, most facilities are distributed where the LPI = 0. For example, 11.2% of light rail transit facilities and 5.0% of sewage pipelines are distributed in areas with low level of liquefaction severity. Moreover, 7.0% of bridges, 9.2% of light rail transit facilities, 5.4% of roadways, and 6.2% of buildings are distributed in areas with high level of liquefaction severity, whereas only 0.1% of roadways, sewage pipelines, and buildings are distributed in areas with very high level of liquefaction severity. Table 5 shows the ratios of facilities corresponding to various LPI ranges for the M_w = 5.0 earthquake. As the earthquake magnitude increases from 5.0 to 6.5, the risk levels of facilities increase. Notably, 93.3% of tunnels, 25.7% of light weight transit facilities, and 6.7% to 31.2% of other facilities are in areas with very low level of liquefaction severity. The facilities with both low and very high level of liquefaction severity comprise approximately 10% of the study area. The length of light weight transit in areas with very high level of liquefaction severity is approximately 7.0 km (28.6%), and is longer than 6.3 km (25.7%) in areas with very low level of liquefaction severity. Table 6 shows the ratios of facilities corresponding to various level of liquefaction severity ranges for the M_w = 6.5 earthquake.

Table 5. Ratios of facilities covered by LPI for M_w = 5.0 earthquake

Facility \ LPI	0	0-5	5-15	15-100
Tunnel, number (%)	15 (100)	0 (0.0)	0 (0.0)	0 (0.0)
Bridge, number (%)	369 (89.6)	14 (3.4)	29 (7.0)	0 (0.0)
Light rail transit, km (%)	19.6 (79.6)	2.8 (11.2)	2.2 (9.2)	0.0 (0.0)
Railway, km (%)	91.3 (100.0)	0.0 (0.0)	0.0 (0.0)	0.0 (0.0)
Road, km (%)	1,041.2 (90.9)	41.2 (3.6)	61.8 (5.4)	1.1 (0.1)
Water pipeline, km (%)	1,181.9 (88.2)	48.2 (3.6)	109.9 (8.2)	0.0 (0.0)
Sewage pipeline, km (%)	1,357.8 (90.4)	75.1 (5.0)	67.6 (4.5)	1.5 (0.1)
Public facility, number (%)	86,862 (89.8)	3,772 (3.9)	5,997 (6.2)	98 (0.1)
Shelter outside a building, number (%)	24 (88.9)	1 (3.7)	2 (7.4)	0 (0.0)

Table 6. Ratios of facilities covered by LPI for M_w = 6.5 earthquake

Facility \ LPI	0	0-5	5-15	15-100
Tunnel, number (%)	14 (93.3)	0 (0.0)	1 (6.7)	0 (0.0)
Bridge, number (%)	278 (67.5)	68 (16.5)	25 (6.1)	41 (9.9)
Light rail transit, km (%)	6.3 (25.7)	2.8 (11.5)	8.5 (34.2)	7.0 (28.6)
Railway, km (%)	76.2 (83.5)	14.5 (15.9)	0.6 (0.6)	0.0 (0.0)
Road, km (%)	714.5 (62.4)	189.5 (16.6)	117.8 (10.3)	123.5 (10.7)
Water pipeline, km (%)	863.4 (64.4)	188.0 (14.1)	143.6 (10.7)	145.0 (10.8)
Sewage pipeline, km (%)	874.2 (58.2)	242.6 (16.1)	205.6 (13.7)	179.6 (12.0)
Public facility, number (%)	62,777 (64.9)	11,414 (11.8)	10,930 (11.3)	11,608 (12.0)
Shelter outside a building, number (%)	16 (59.3)	6 (22.2)	1 (3.7)	4 (14.8)

https://doi.org/10.5194/nhess-2021-287
Preprint. Discussion started: 21 October 2021

5 Results and discussion

Liquefaction phenomena were found during the Pohang earthquake in 2017. In this study, the risk levels of facilities associated with earthquake-induced liquefaction were examined for earthquake magnitudes of 5.0 and 6.5 in Kimhae City. The results are as follows.

1. Areas with very low level of liquefaction severity for an earthquake magnitude of 5.0 cover 94% (433.5 km^2) of the total area in Kimhae City. Level of liquefaction severity from high to very high are distributed in the Daedong-myun area, which consists of soft soil layers.

2. Areas with very low and high level of liquefaction severity for an earthquake magnitude of 6.5 cover 83% (381.4 km^2) and 2.5% (11.5 km^2) of the total area, respectively. As the earthquake magnitude changes from 5.0 to 6.5, the proportions of very low and high level of liquefaction severity are 11.3% and 2.3%, respectively, whereas the proportions of low and very high level of liquefaction severity are 7.6% (35.1 km^2) and 6.0% (27.7 km^2), respectively. Moreover, the level of liquefaction severity changes from very low to low and from high to very high. Most of the areas have low level of liquefaction severity for the earthquake magnitude of 5.0, whereas some change to very high level of liquefaction severity for the earthquake magnitude of 6.5. This indicates that an M_w = 6.5 earthquake may result in higher risks levels for facilities associated with high level of liquefaction severity.

3. The areas with high level of liquefaction severity for the earthquake magnitude of 5.0 cover less than 0.1% of roadways, sewage pipelines, and public facilities. In addition, 80% of facilities (except light rail transit facilities) correspond to very low level of liquefaction severity. Therefore, the liquefaction-induced risk levels for facilities are very low for the M_w = 5.0 earthquake. However, as the earthquake magnitude increases to 6.5, 9% of facilities (except for tunnel and railway facilities) and 30% of light rail transit facilities are distributed in high level of liquefaction severity areas, reflecting higher risk levels for these facilities.

4. The SPT database for Kimhae City was used to estimate the CSR and LPI. Higher LPI values are found at the sedimentary layers of soils widely distributed adjacent to Nakdong river. Importantly, a magnification of ground movement occurs near the fault zone during an earthquake. Therefore, the construction of buildings in regions with high liquefaction severity should be avoided.

Acknowledgements. This work was supported by the 2019 INJE University research grant.

References

Bakir, D., Karasin, I. B.: Damage according to liquefaction and suggestions, ISOR J. Eng., 6, 1-6, 2016.

Ballegooy, S., Malan, P. J., Jacka, M. E., Lacrosse, V.I.M.F., Leeves, J.R., Lyth, J.E., Cowan, H.: Methods for characterizing effects of liquefaction in terms of damage severity, 15th World Conference on Earthquake Engineering, Lisbon, Portugal, 24-28 September, 1-10, 2012.

Bhattacharya, S. Hyodo, M., Goda, K., Tazoh, T., Taylor, C.A.: Liquefaction of soils in the Tokyo Bay area from the 2011 Tohoku (Japan) earthquake", Soil Dynamics Eng., 31, 1618-1628, 2011.

Bray J. D., Dashti S.: Liquefaction-induced movements of buildings with shallow foundations, 5th International Conference on Recent Advances in Geotechnical Earthquake Engineering and Soil Dynamics, 26 May, Sandiego, CA, 1-19, 2010.

Bullock, Z., Porter, K., Liel, A., Dashti, S.: A framework for the evaluation of liquefaction consequences for shallow-founded structures, 13th International Conference on Applications of Statistics and Probability in Civil Engineering, Seoul, South Korea, May 26-30, 1-8, 2019.

Choe, J.S., Ku, T.J.: A study on mapping of Liquefaction Hazard at a Megalopolis in Korea, International Symposium on Urban Geotechnics, Proceedings of the Korean Geotechnical Society Conference, 25-26, 2009.

Choi, I.K., Masato, N., Choun, Y.S., Yasuki, O., Yun, K.-H.: Study on the earthquake ground motion attenuation characteristics

https://doi.org/10.5194/nhess-2021-287
Preprint. Discussion started: 21 October 2021

Natural Hazards and Earth System Sciences
Discussions

in Korea and Japan using 2005 Fukuoka earthquake record, J. Earthquake Eng. in Korea, 10, 45-54, 2005.

Chung, J.W., Rogers, J.D.: Simplified method for spatial evaluation of liquefaction potential in the St. Louis area, J. Geotech. and Geoenv. Eng., 137, 505-515, 2011.

Cubrinovski, M., Bradley, B., Wotherspoon, L., Green, R., Bray, J., Wood, C., Pender, M., Allen, J., Bradshaw, A., Rix, G.: Geotechnical aspects of the 22 February 2011 Christchurch earthquake, Civil & Natural Resources Engineering, University of Canterbury & Christchurch, 2011.

Eidinger, J., C.A Davis: Recent earthquakes: implications for US water utilities, Water Research Foundation, 2012.

Habibullah, B. Md., Pokhrel, R. M., Tachibana, S.: GIS-based soil liquefaction hazard zonation due to earthquake using geotechnical data, Int. J. GEOMATE, 2, 154-160, 2012.

Hayden, C. P.: Liquefaction-induced building performance and near-fault ground motions, Ph.D. Thesis, University of California, Berkeley, Fall 2014.

Holzer, T.L.: Probabilistic liquefaction hazard mapping, Proc., 4th Conference. on Geotechnical Earthquake Engineering and Soil Dynamics, ASCE, Sacramento, CA., 1-32, 2008.

Iwasaki, T., K. Tokida, F. Tatsuoka, S. Watanabe, S. Yasuda, H. Sato: Microzonation for soil liquefaction potential using simplified methods, Proc., 3rd Int. Conf. on Microzonation, Seattle, WA, 1319-1330, 1982.

Jo, N.D., Baag, C.E.: Estimation of spectrum decay parameter x and stochastic prediction of strong ground motions in southeastern Korea, J. Earthquake Eng. in Korea, 7, 59-70, 2003.

Kamao, S., Takezawa, M., Yamada, K., Jinno, S., Shinoda, T., Fukazawa, E.: A study of earthquake-caused liquefaction the case of Urayasu City, WIT Transactions on State of the Art in Science and Engineering, 79, 149-161, 2014.

Kramer, S.L.: Geotechnical earthquake engineering. Prentice Hall Upper Saddle River. NJ, Standford Center for Induced and Triggered Seismicity, Stanford University, CA, 1996.

Lanzano, G., Magistris, F. S., Salzano, E., Fabbrocino, G.: Vulnerability of Industrial Components to Soil Liquefaction, Chemical Engineering Transactions, Vol. 36, 421-426, 2014.

Lee, D.H., Ku, C.S., Yuan, H.: A study of the liquefaction risk potential at Yuanlin, Taiwan, Engineering Geology, 71, 97-117, 2003.

Lu, C.-C., Hwang, J.-H., Hsu, S.-Y.: The impact evaluation of soil liquefaction on low-rise building in the Meinong earthquake, Earth, Planets and Space, 69, 1-16, 2017.

Midorikawa, S., Ohtake, Y.: Variance of peak Ground Acceleration and velocity in attenuation relationship, 13th World Conference on Earthquake Engineering, Vancouver, B.C., Canada, 1-10, Aug. 2004.

Munson, C.G.: Analysis of the attenuation of strong ground motion on the island of Hawaii, Bulletin of the Seismological Society of America, 87, 945–960. 1997.

Naik, S. P., Gwon, O., Park, K., Kim Y.-S.: Land damage mapping and liquefaction potential analysis of soils from the epicentral region of 2017 Pohang Mw 5.4 earthquake, South Korea, Sustainability, 12, 1-21, 2020.

O'Rourke, T.D., Jeon, S.-S., Toprak, S., Cubrinovski, M., Hughes, M., van Ballegooy, S., Bouziou, D.: Earthquake response of underground pipeline networks in Christchurch, NZ, Earthquake Spectra, 30, 183-204, 2014.

Seed, H.B., Idriss, I.M.: Ground motions and soil liquefaction during earthquake, Earthquake Engineering Research Institute Monograph, Oakland, CA, 1982.

Wakamatsu, K., Numata, A.: Effect of liquefaction susceptibility on building damage during the 1995 Kobe earthquake, ISOR Journal of Engineering, 6, 1-6, 2016.

Youd, T.L., Idriss, I.M.: Liquefaction resistance of soils: Summary Report from the 1996 NCEER and 1998 NCEER/NSF Workshops on Evaluation of Liquefaction Resistance of Soils, Journal of Geotechnical and Geoenvironmental Engineering, 127, 817-833, 2001.

Ziabari S. H., Ghafoori M., Moghaddas, N. H., Lashkaripour G. R.: Liquefaction potential evaluation and risk assessment of existing structures: A case study in Astaneh-ye Ashrafiyeh City, Iran, Eur Asian Journal of BioSciences, 11, 52-62, 2017.

Zupan, J. D.: Seismic performance of buildings subjected to soil liquefaction, Ph.D. Thesis, University of California, Berkely, 2014.